Supplementary Information

Patchy Stereocomplex Micelles as Efficient Compatibilizers for Polymer Blends

Roman Schaller,[a] Marius Schmidt,[a] Kristian Schweimer[b,c] and Holger Schmalz[a,d]*

R. Schaller, M. Schmidt, Dr. Kristian Schweimer, Dr. H. Schmalz

[a] Macromolecular Chemistry, University of Bayreuth, Universitätsstraße 30, 95447 Bayreuth (Germany)

[b] Biochemistry IV, Biophysical Chemistry, University of Bayreuth, Universitätsstraße 30, 95447 Bayreuth (Germany)
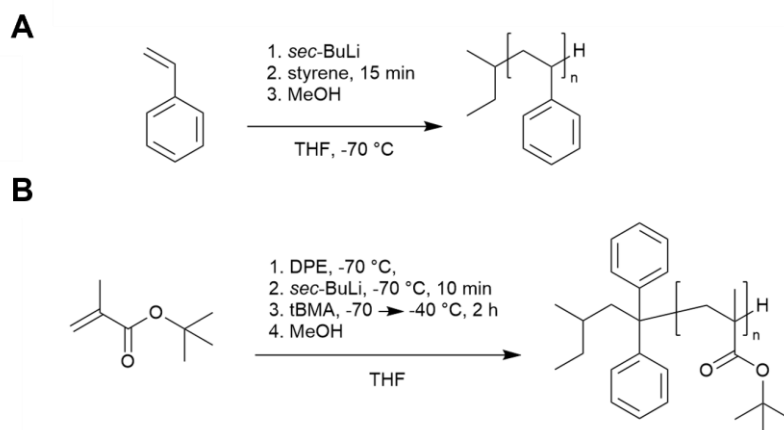
[c] Northern Bavarian NMR Center, University of Bayreuth, Universitätsstraße 30, 95447 Bayreuth (Germany)

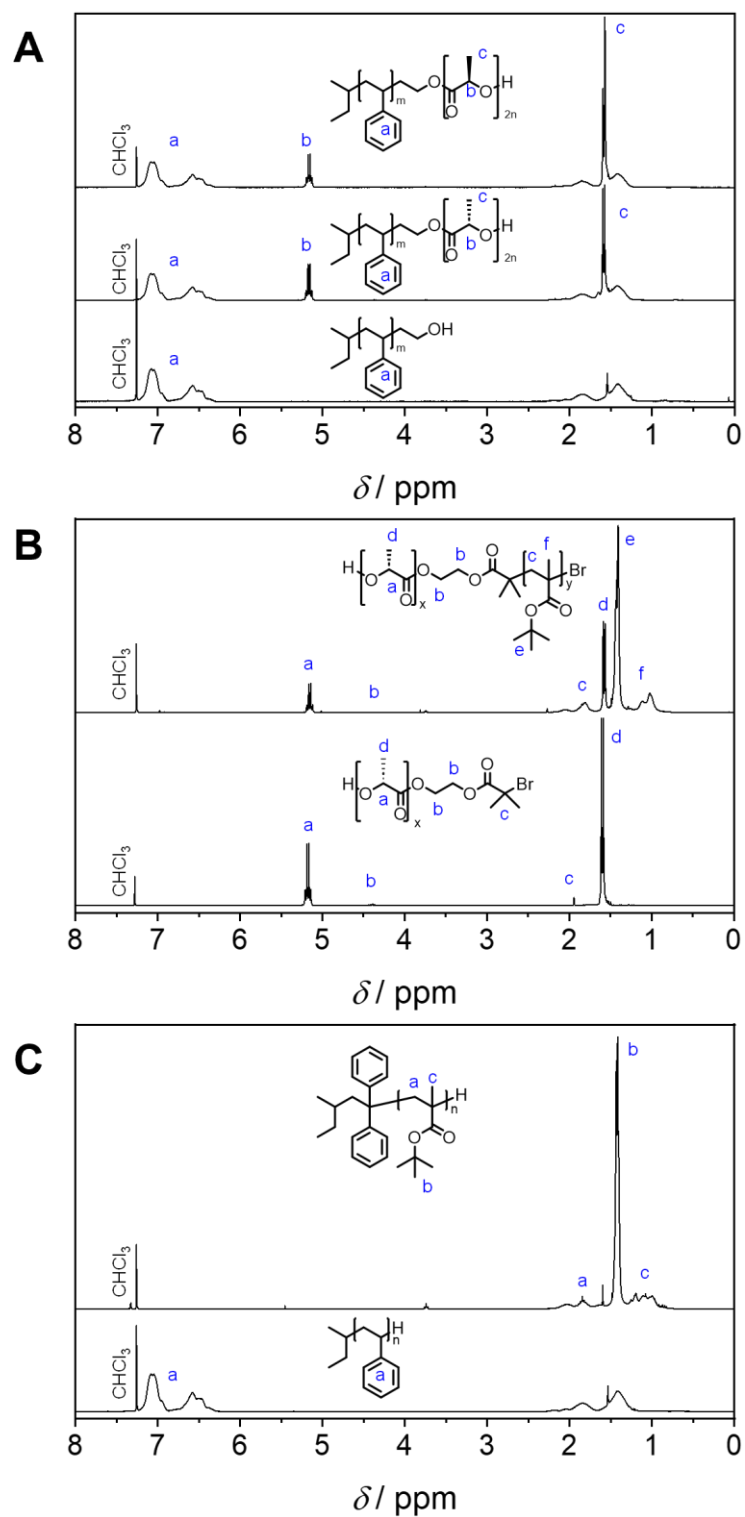[d] Bavarian Polymer Institute, Universitätsstraße 30, 95447 Bayreuth (Germany)

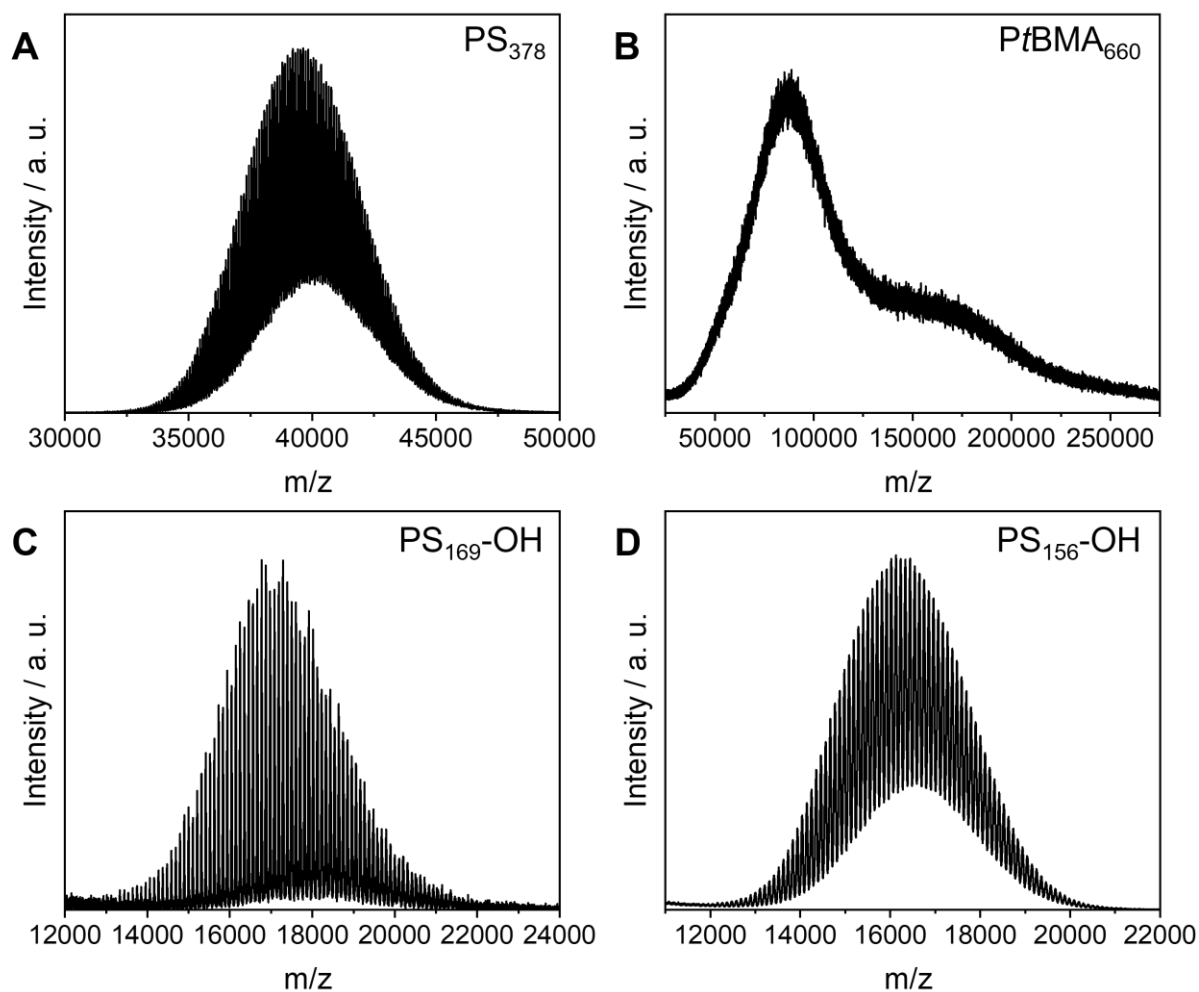E-mail: holger.schmalz@uni-bayreuth.de
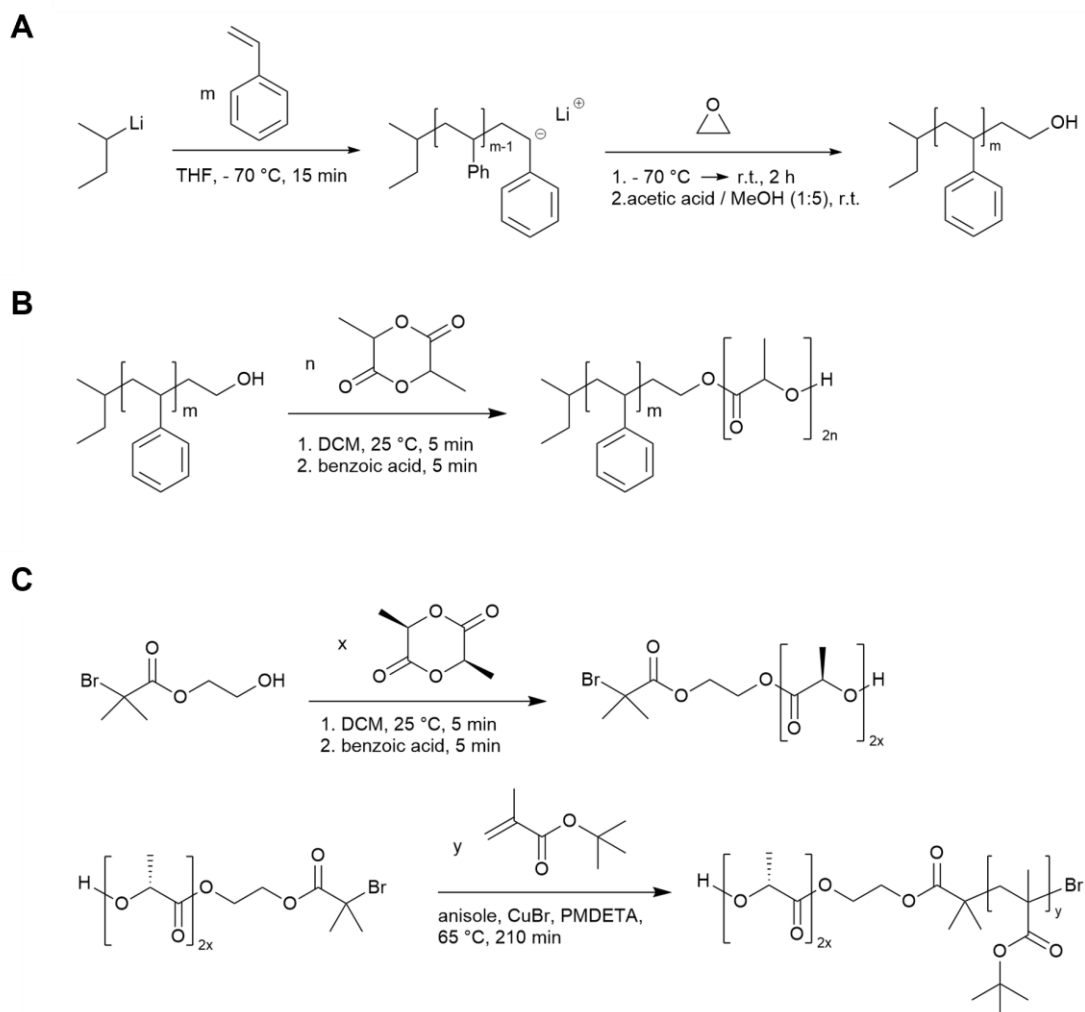
Scheme S1: Synthesis of A) PS-OH, B) PS-*b*-P*L*LA or PS-*b*-P*D*LA and C) P*D*LA-*b*-P*t*BMA diblock copolymers.

Scheme S2: Synthesis of A) PS and B) P*t*BMA homopolymers by living anionic polymerization.

Fig. S1: ^{1}H NMR (CDCl$_3$, 300 MHz) spectra of A) PS-OH, PS-*b*-P*L*LA, PS-*b*-P*D*LA, B) P*D*LA-Br, P*D*LA-*b*-P*t*BMA and C) PS, P*t*BMA.

Fig. S2: MALDI-ToF MS spectra of A) PS, B) P*t*BMA (the shoulder at higher molecular weights is an artifact arising from the combination of two polymer chains with one cation), C) PS$_{169}$-OH and D) PS$_{156}$-OH (PS samples: DCTB, AgTFA; P*t*BMA: DCTB, NaTFA).

**Table S1**: Molecular characteristics of synthesized polymers.

Sample	Composition (wt% / DP)[a]	M_n(NMR)[a] [g mol^{-1}]	M_n(SEC)[b] [g mol^{-1}]	$Đ$[b]	M_n(MS)[c] [g mol^{-1}]	$Đ$[c]
PS	- / S$_{378}$	-	41 500	1.05	39 400	1.0
PtBMA	- / tBMA$_{660}$	-	87 000	1.06	93 700	1.06
PS$_{169}$-OH	- / S$_{169}$EO$_1$	-	19 600	1.06	17 600	1.0
PS$_{156}$-OH	- / S$_{156}$EO$_1$	-	16 600	1.06	16 300	1.0
PDLA$_{100}$-Br	- / DLA$_{100}$	7 500	13 500	1.16		
PDLA$_{62}$-Br	- / DLA$_{62}$	4 600	6 300[d]	1.09[d]		
PDLA$_{62}$-RB	- / DLA$_{62}$RB$_1$	5 200	6 700[d]	1.10[d]		
PS-b-PLLA	S$_{70}L$LA$_{30}$ / S$_{169}L$LA$_{106}$	25 300	27 900	1.08		
PS-b-PDLA	S$_{68}D$LA$_{32}$ / S$_{156}D$LA$_{106}$	24 000	30 000	1.07		
PS-b-PLLA-Br	S$_{72}L$LA$_{28}$ / S$_{169}L$LA$_{96}$	24 500	27 900	1.10		
PDLA-b-PtBMA	DLA$_{28}t$BMA$_{72}$ / DLA$_{100}t$BMA$_{132}$	26 200	35 100	1.19		
PS-b-PLLA-b-PtBMA	S$_{33}L$LA$_{13}$T$_{54}$ / S$_{169}L$LA$_{96}$T$_{200}$	52 600	42 200	1.18		

a) determined from ^{1}H NMR (CDCl$_3$, 300 MHz) using the ATRP end group or absolute M_n of the PS and PDLA precursor polymers (determined by MALDI-ToF MS or ^{1}H NMR spectroscopy) for internal signal calibration, respectively (DP = degree of polymerization)
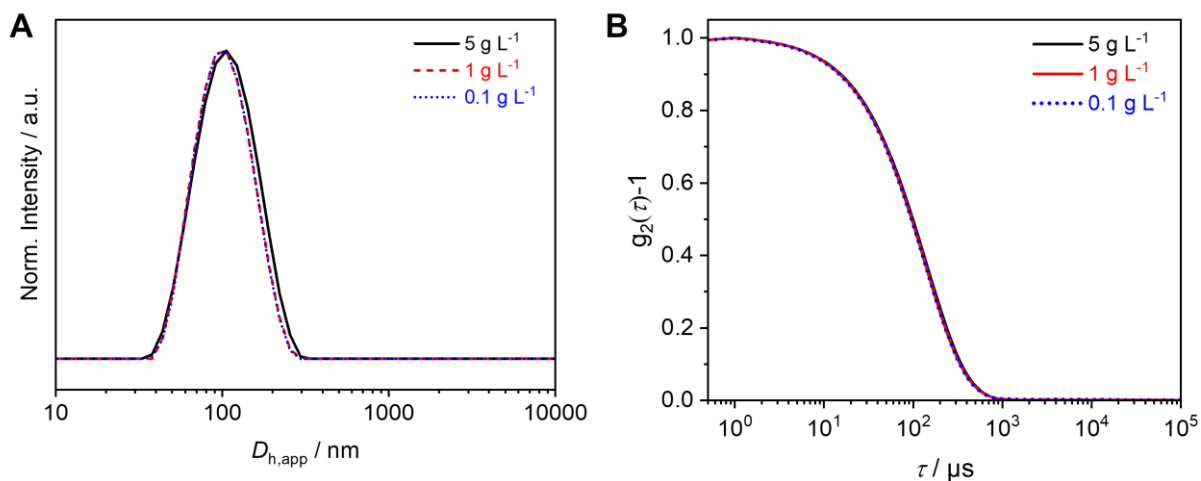
b) determined from CHCl$_3$-SEC (PS calibration), $Đ$ = molar mass dispersity

c) determined from MALDI-ToF MS

d) determined from THF-SEC (PS calibration)
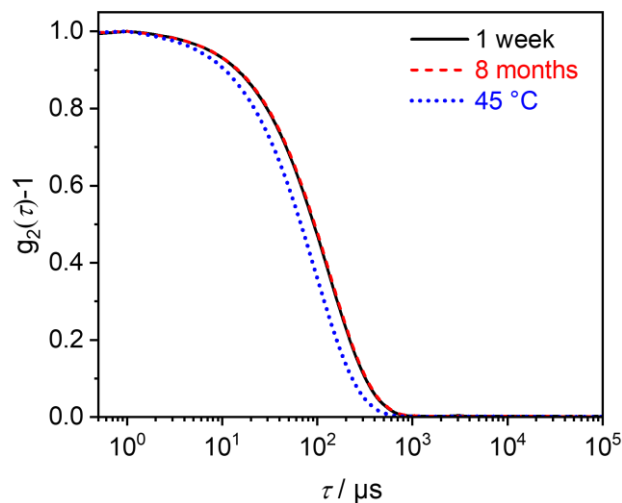
Fig. S3: Autocorrelation functions from DLS for SC micelles prepared from PS-*b*-P*L*LA/P*D*LA-*b*-P*t*BMA mixtures ($c = 5$ g L^{-1}, CH) after aging for 1 week, 8 months, and at 45 °C.

Fig. S4: DLS measurements of SC micelles in CH prepared from PS-*b*-P*L*LA/P*D*LA-*b*-P*t*BMA mixtures with a concentration of $c = 5$ g L^{-1} and upon further dilution to $c = 1$ and 0.1 g L^{-1}. A) Hydrodynamic diameter distributions and B) autocorrelation functions.
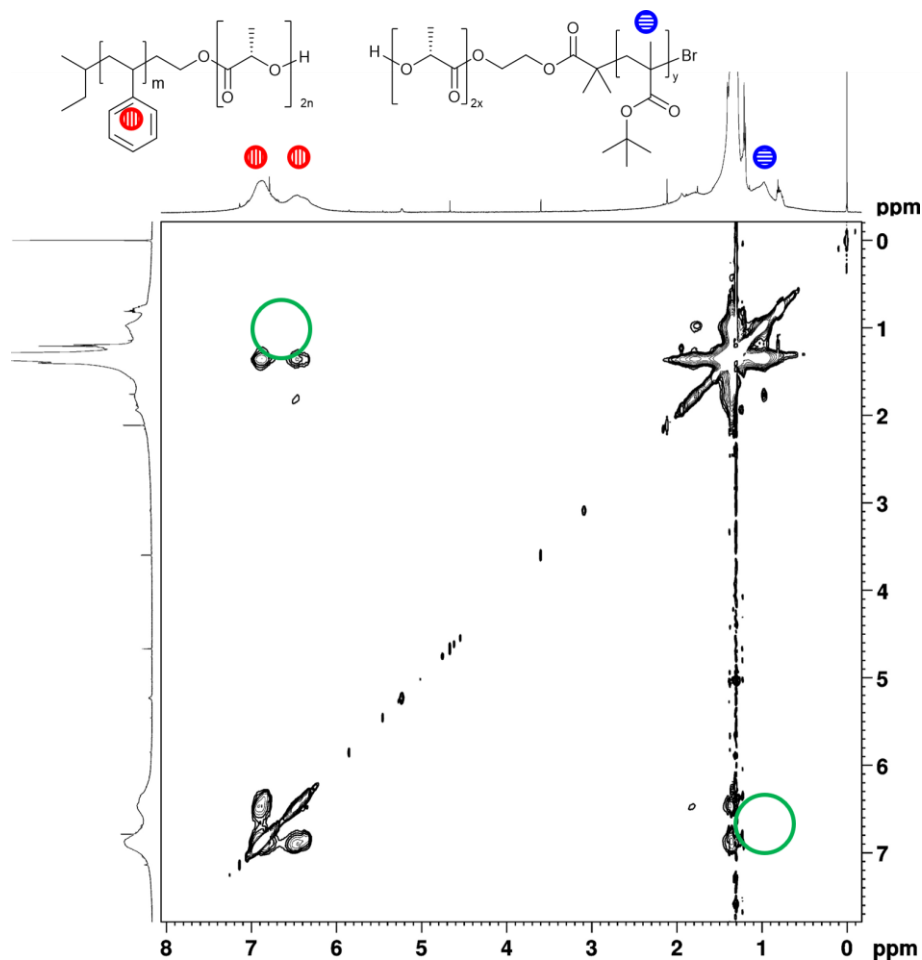
Fig. S5: Contour plot of a 2D ^{1}H NOESY experiment on a SC micelle dispersion prepared from PS-*b*-P*L*LA/P*D*LA-*b*-P*t*BMA mixtures (c = 5 g L^{-1}, CH-d_{12}). The green circles indicate the positions where cross-peaks would be expected in case of a mixed PS/P*t*BMA corona. In a mixed corona, the PS and P*t*BMA segments would be in close proximity, giving rise to magnetization transfer by cross-relaxation. Hence, the absence of those cross-peaks confirms that the microphase separation within the PS/P*t*BMA corona of the SC micelles is present already in the dispersed state.
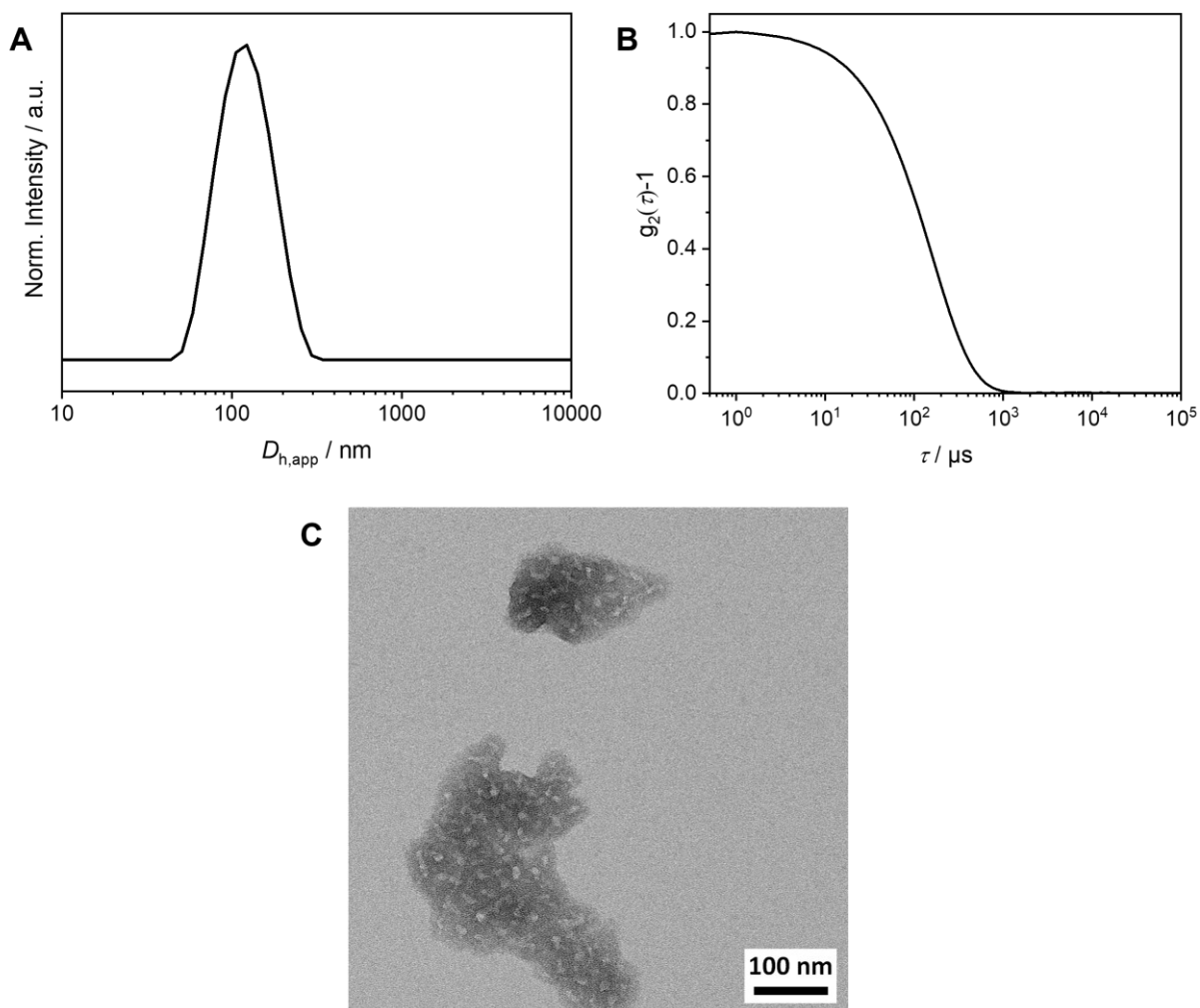
Fig. S6: A) Hydrodynamic diameter distribution and B) autocorrelation function of a PS-*sc*-PLA-PS micelle dispersion in CH ($c = 5.0$ g L^{-1}) determined by DLS. C) TEM micrograph of the respective micelles. The dispersion was prepared by adding a mixture of PS-*b*-P*L*LA and PS-*b*-P*D*LA in DCM ($V = 2$ mL, $c = 50$ g L^{-1}) to CH ($V = 18$ mL), subsequent evaporation of DCM and refilling with CH. PS was selectively stained with RuO$_4$ vapor and appears dark.
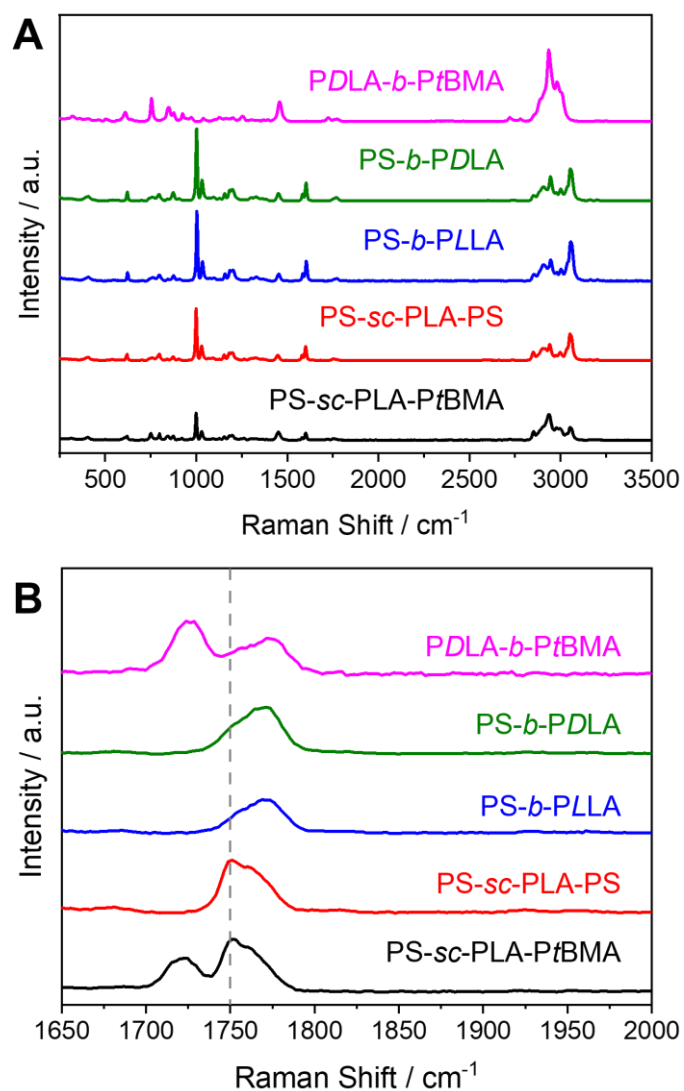
Fig. S7: Raman spectra of employed diblock copolymers and dried SC micelles. A) Full spectra and B) zoom-ins of the carbonyl stretching vibration regime (dashed line indicates location of SC specific band).
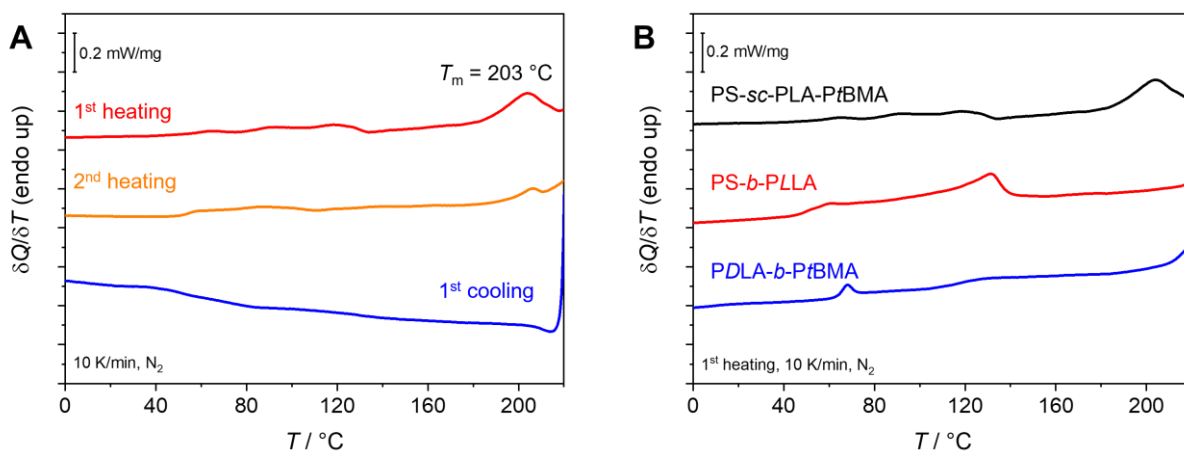
Fig. S8: A) DSC measurements of freeze-dried PS-*sc*-PLA-P*t*BMA micelles. B) 1st heating traces of freeze-dried PS-*sc*-PLA-P*t*BMA micelles and the respective diblock copolymers used for their preparation.
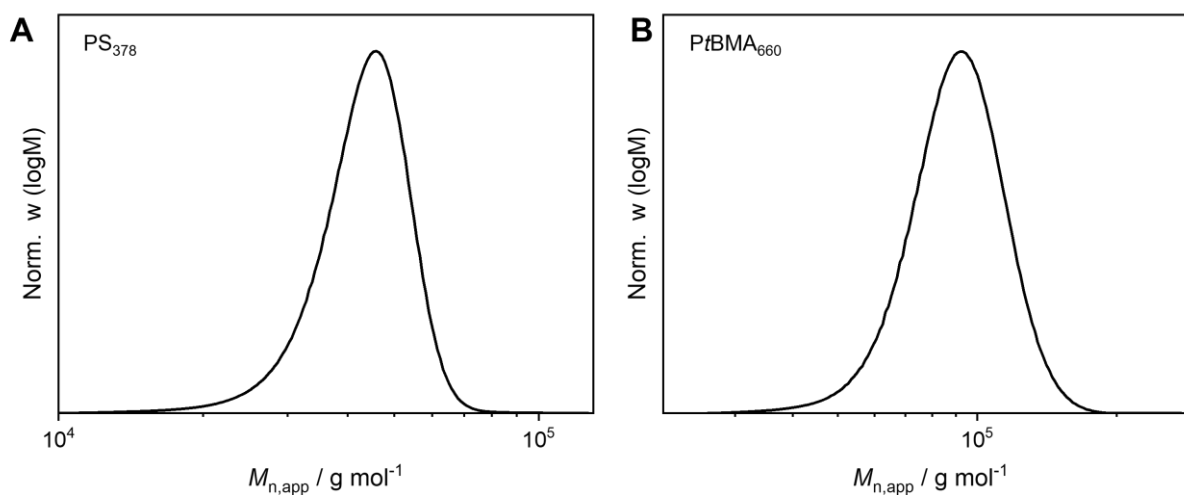

Fig S9: Apparent molecular weight distributions of A) PS and B) P*t*BMA homopolymers (CHCl$_3$-SEC, PS calibration).
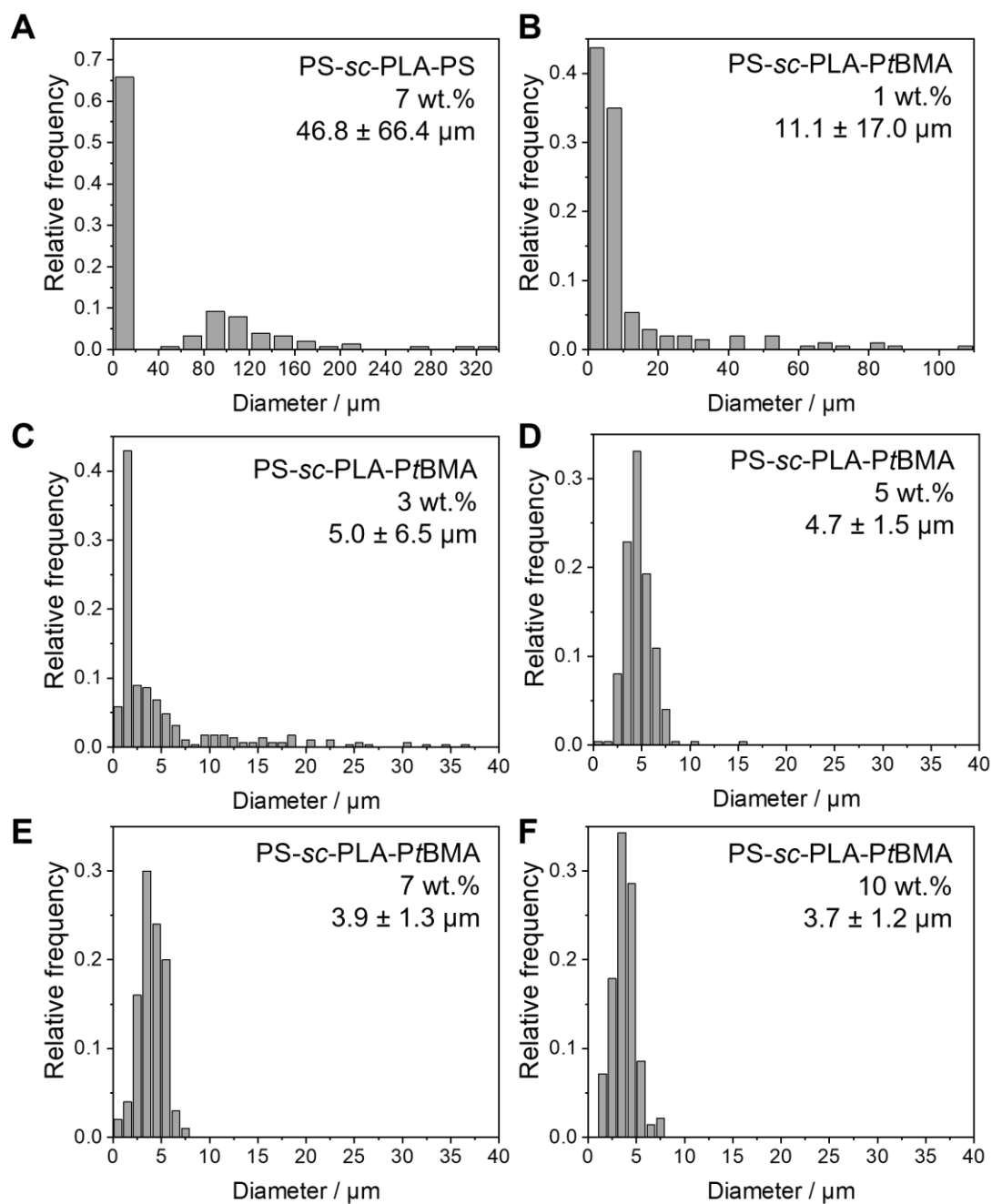
Fig. S10: Histograms of PS droplet diameter distributions determined by Raman imaging of PS/P*t*BMA (30/70 (w/w)) blends compatibilized with A) 7 wt% PS-*sc*-PLA-PS micelles or different amounts of patchy PS-*sc*-PLA-P*t*BMA micelles: B) 1, C) 3, D) 5, E) 7 and F) 10 wt%. For size evaluation at least 100 PS domains from different positions were counted.
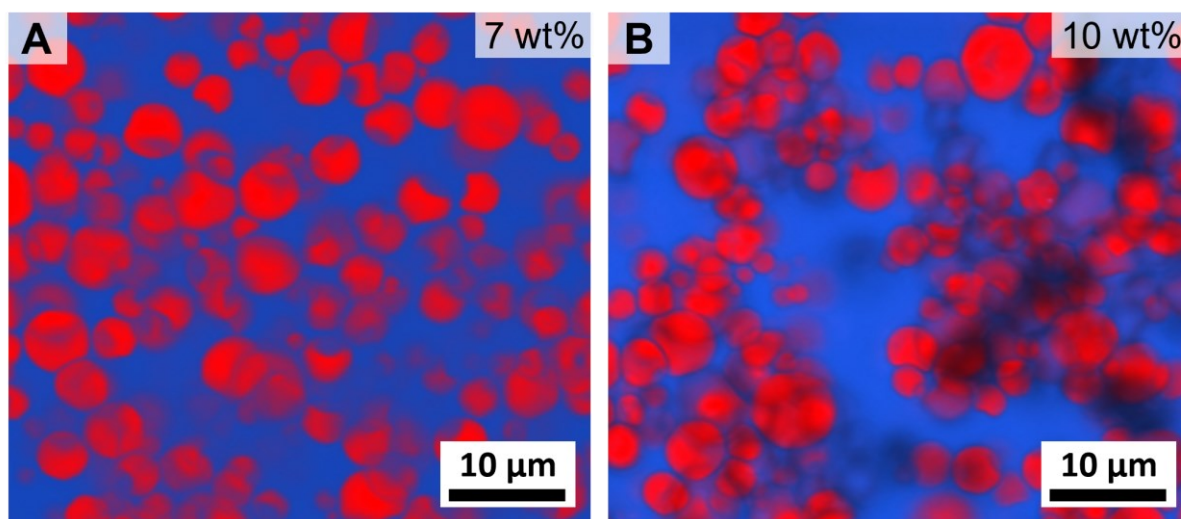
Fig. S11: Spatial component distribution at higher magnification extracted from Raman imaging for PS/P*t*BMA (30/70 (w/w)) blends compatibilized with A) 7 wt% and B) 10 wt% patchy PS-*sc*-PLA-P*t*BMA micelles. The domains colored in red represent PS droplets being dispersed in a continuous P*t*BMA matrix (depicted in blue).
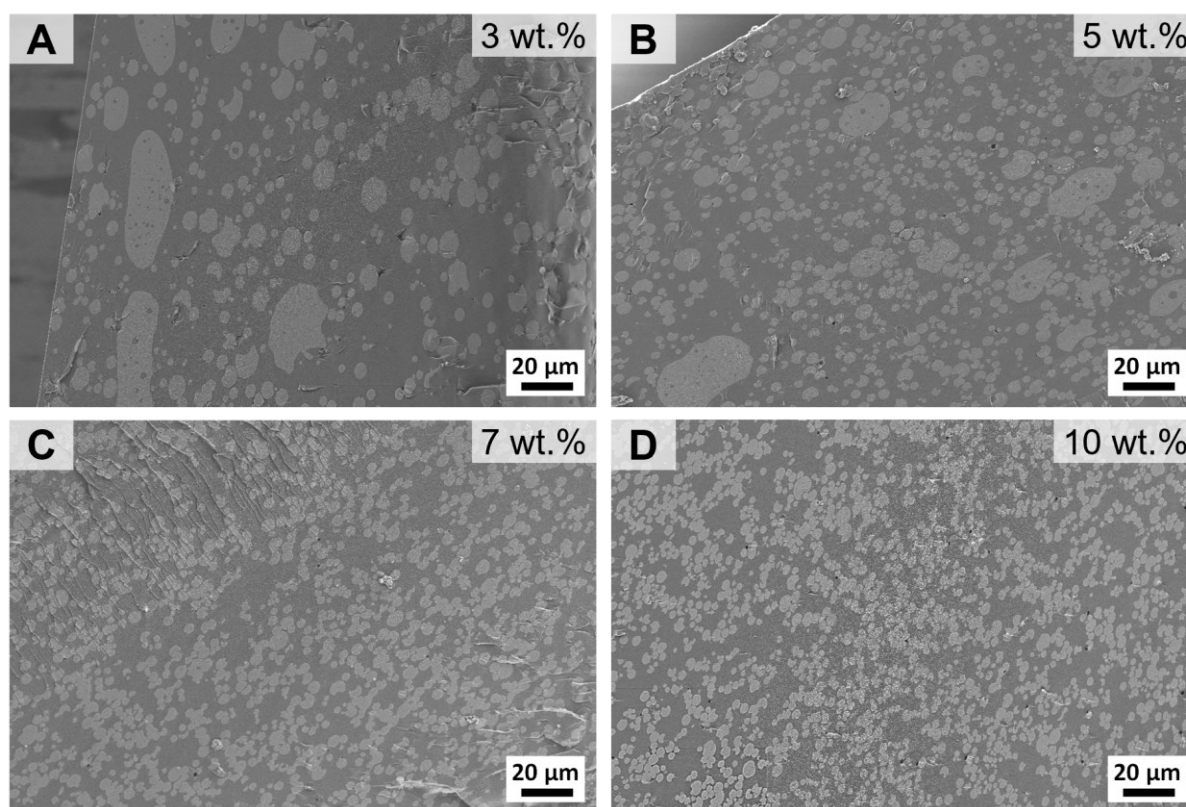

Fig. S12: Overview SEM images of the fracture surfaces of PS/P*t*BMA (30/70 (w/w)) blends compatibilized with A) 3, B) 5, C) 7 and D) 10 wt% patchy PS-*sc*-PLA-P*t*BMA micelles, taken at lower magnification. The PS domains were selectively stained with RuO$_4$ vapor to enhance contrast and appear bright.
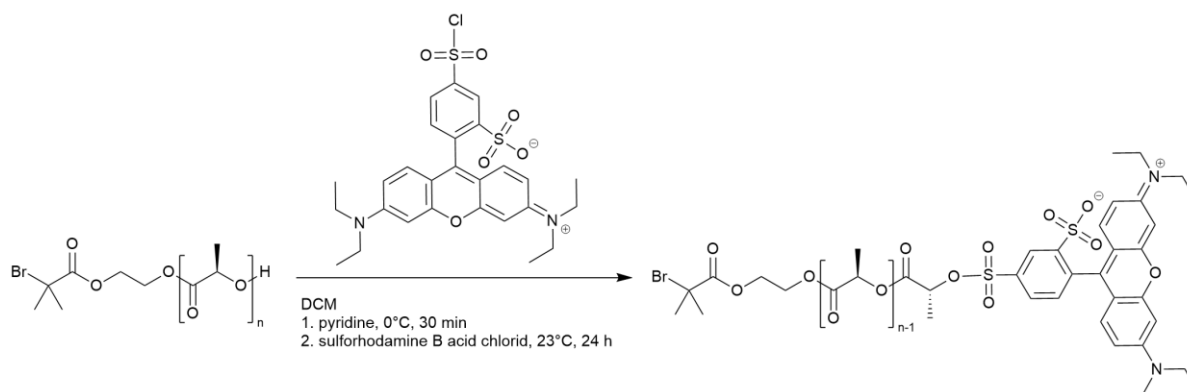
Scheme S3: Synthesis of fluorescently labelled P*D*LA homopolymer (P*D*LA$_{62}$-RB).
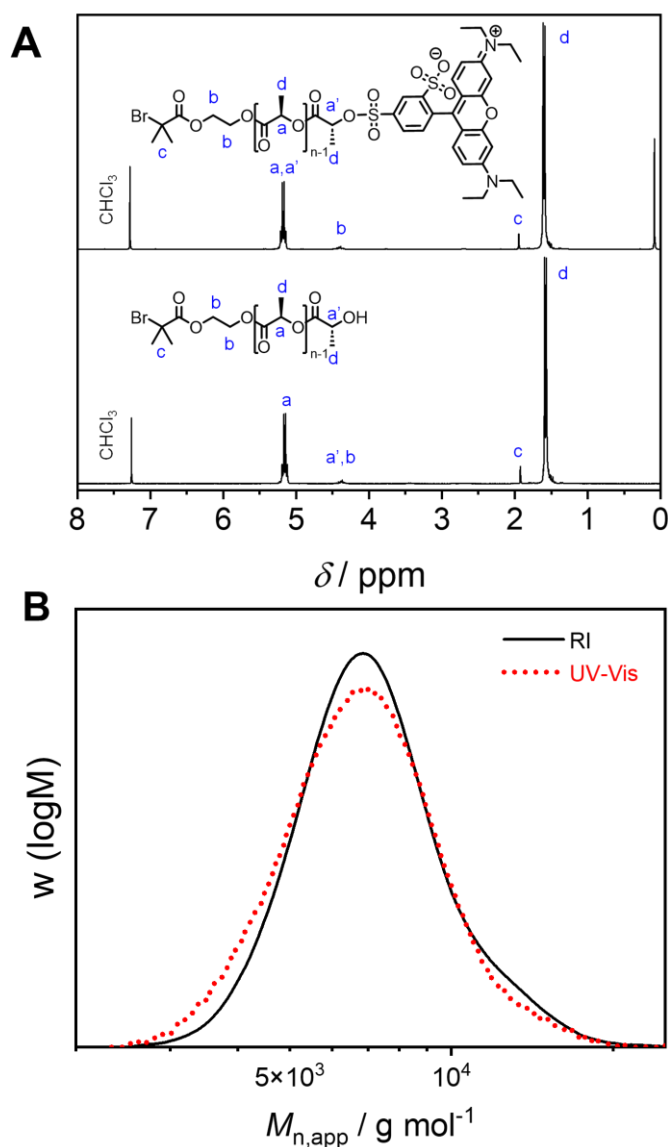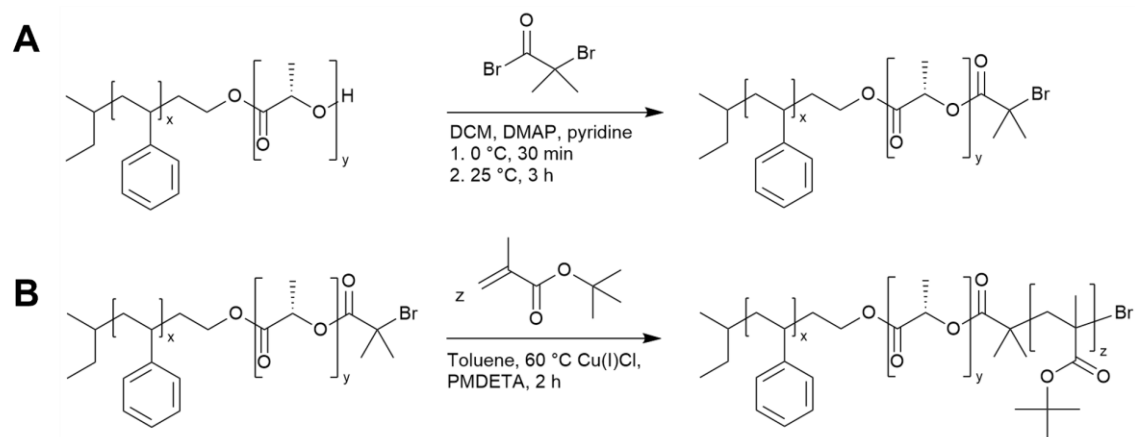

Fig. S13: A) ^{1}H NMR (CDCl$_3$, 300 MHz) spectra of P*D*LA$_{62}$-Br and P*D*LA$_{62}$-RB. B) Apparent molecular weight distributions of P*D*LA$_{62}$-RB (THF-SEC, PS calibration, UV-vis detector at λ = 580 nm). The identical RI and UV-vis traces for P*D*LA$_{62}$-RB prove the successful end-functionalization of P*D*LA$_{62}$ with sulforhodamine B.
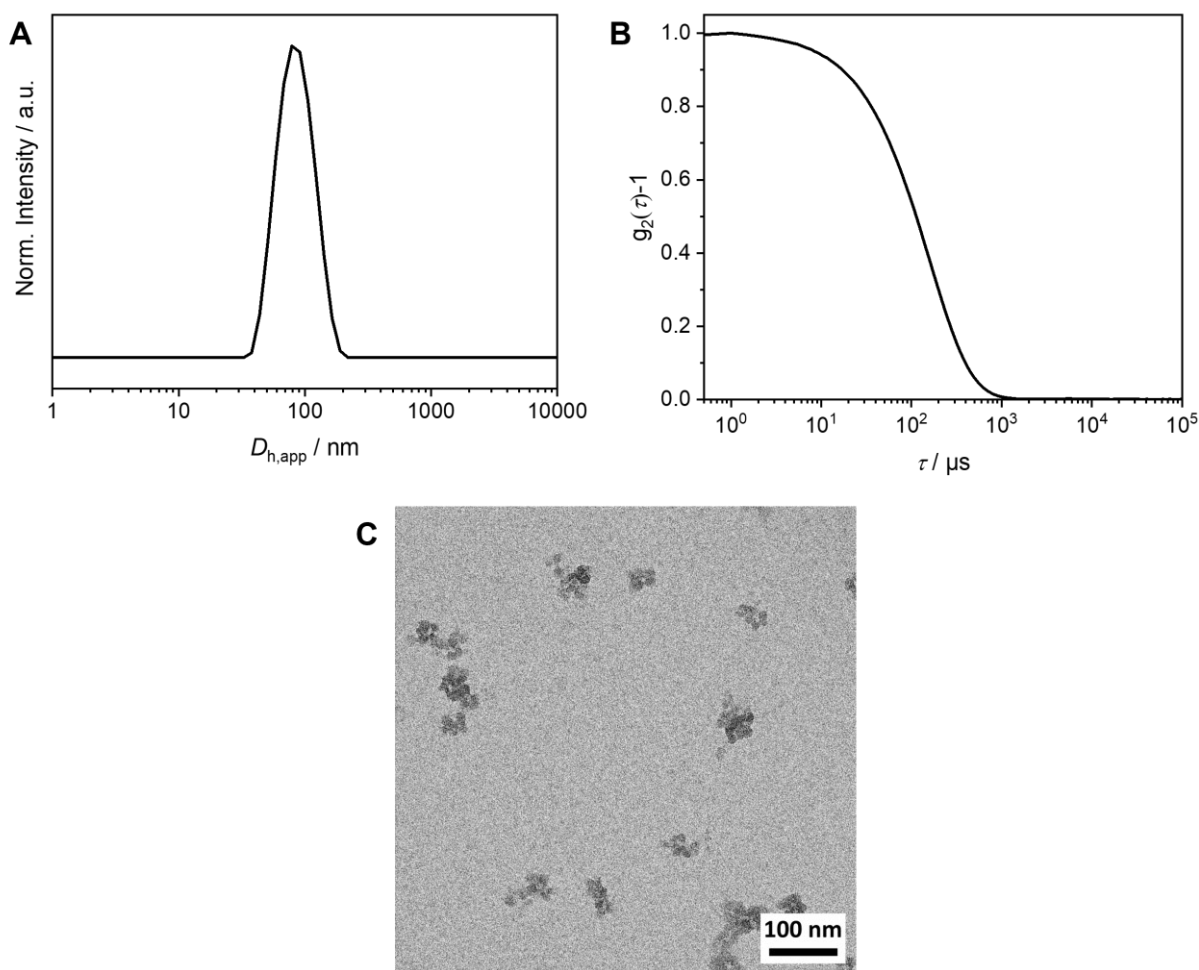
Fig. S14: A) Hydrodynamic diameter distribution and B) autocorrelation function of a PS-*sc*-PLA-P*t*BMA_RB micelle dispersion in CH (c = 1.0 g L^{-1}) determined by DLS. C) TEM micrograph of the respective micelles. The dispersion was prepared by the addition of a mixture of PS-*b*-P*L*LA, PS-*b*-P*D*LA and P*D*LA$_{62}$-RB (10 wt% of total P*D*LA amount) in DCM (V = 300 µL, c = 10 g L^{-1}) to CH (V = 2.7 mL), subsequent evaporation of DCM and refilling with CH. PS was selectively stained with RuO$_4$ vapor and appears dark.
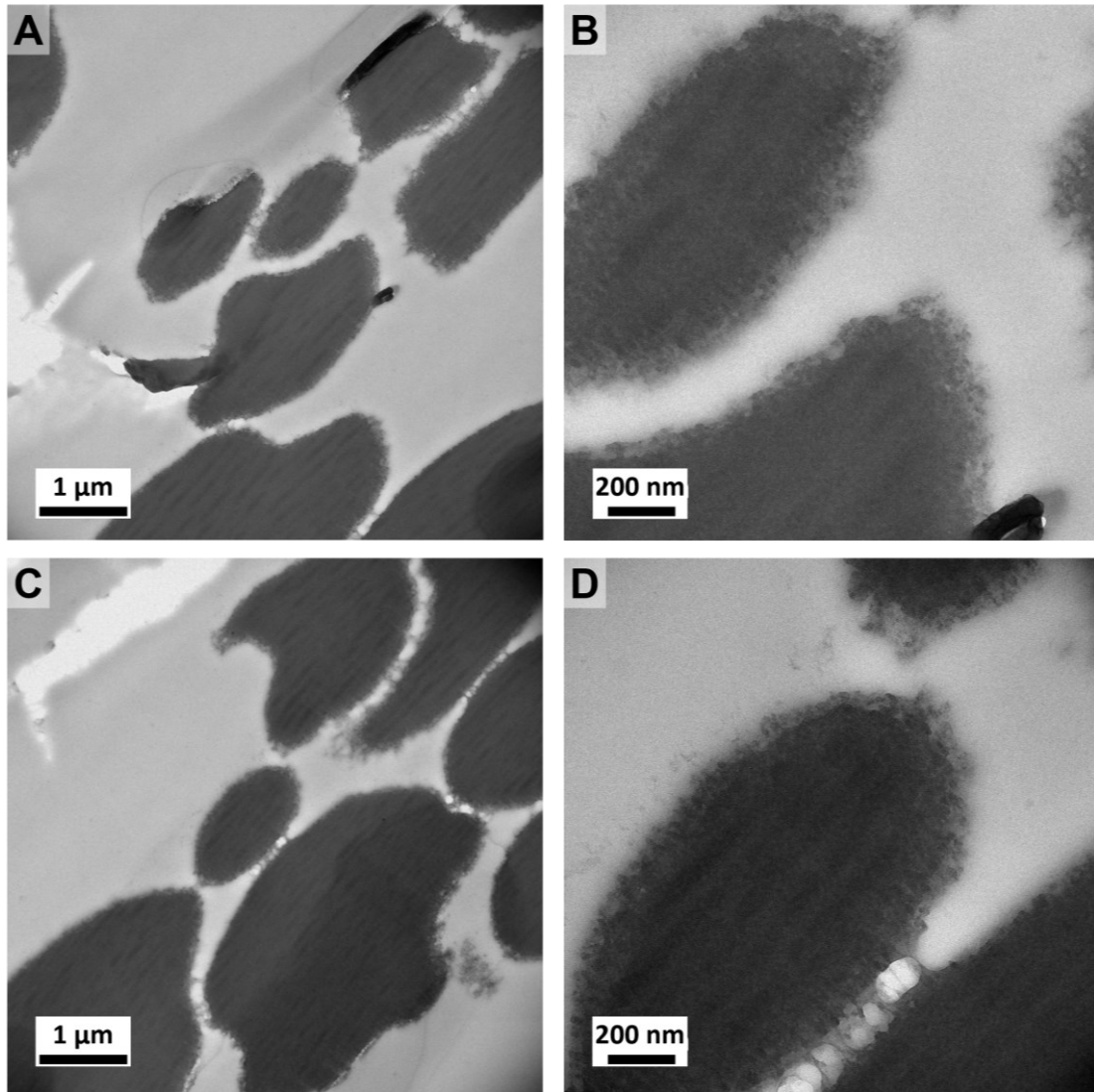
Fig. S15: TEM micrographs of a thin film of a PS/P*t*BMA (30/70 (w/w)) blend compatibilized with 7 wt% patchy PS-*sc*-PLA-P*t*BMA micelles. The PS domains were selectively stained with RuO$_4$ vapor to enhance contrast and appear dark.
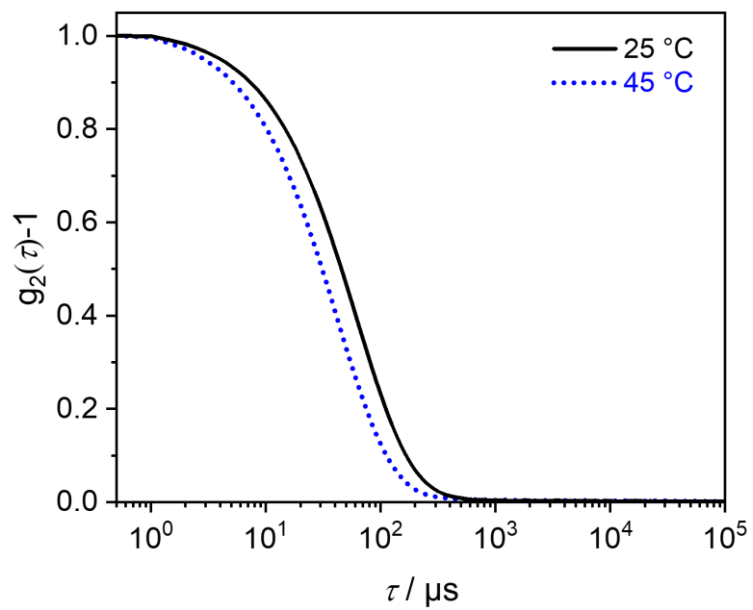
Scheme S4: Synthesis of A) the PS-*b*-P*L*LA-Br diblock copolymer end-functionalized with an ATRP initiating site (S$_{169}$LLA$_{96}$-Br) and B) the PS-*b*-P*L*LA-*b*-P*t*BMA triblock terpolymer (S$_{169}$LLA$_{96}$T$_{200}$).
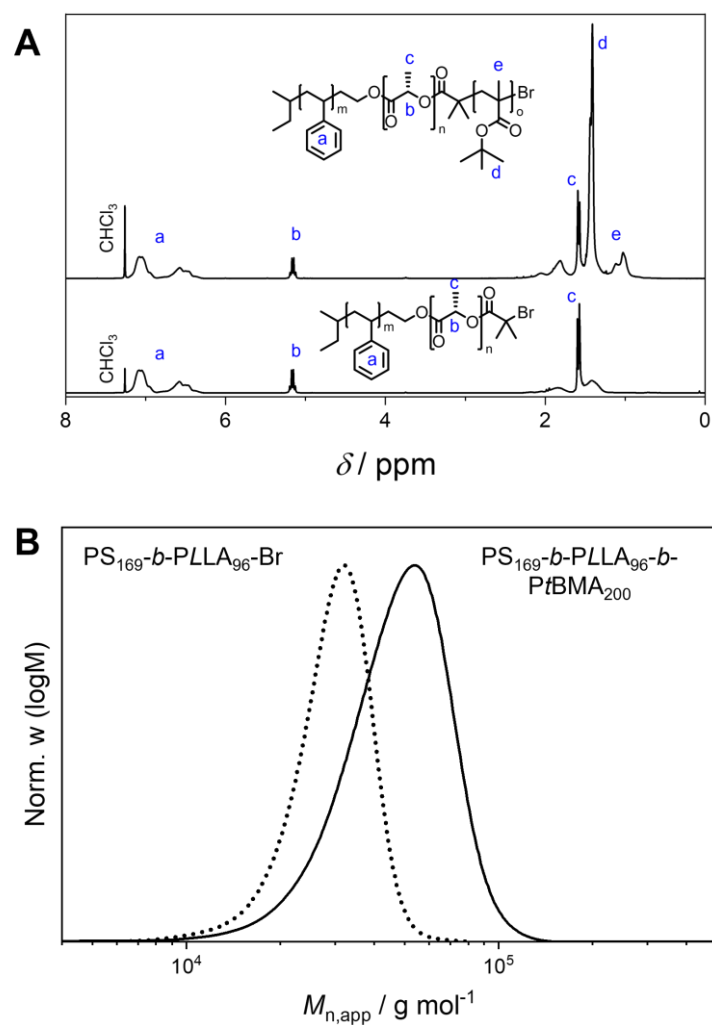
Fig. S16: A) ^{1}H NMR (CDCl$_3$, 300 MHz) spectra and B) apparent molecular weight distributions (CHCl$_3$-SEC, PS calibration) of PS$_{169}$-*b*-P*L*LA$_{96}$-Br and PS$_{169}$-*b*-P*L*LA$_{96}$-*b*-P*t*BMA$_{200}$.

Fig. S17: Autocorrelation functions from DLS for PS-*b*-P*L*LA-*b*-P*t*BMA Janus micelles (c = 5 g L^{-1}, CH) at 25 and 45 °C.